Design of Two Lightweight, High-Bandwidth Torque-Controlled Ankle Exoskeletons

Kirby Ann Witte[1], Juanjuan Zhang[1,2], Rachel W. Jackson[1], Steven H. Collins[1,3,*]

***Abstract*—Lower-limb exoskeletons that can comfortably apply high torques at high bandwidth can be used to probe the human neuromuscular system and assist gait. We designed and built two tethered ankle-foot exoskeletons with strong lightweight frames, comfortable three-point contact with the leg, and series elastic elements for improved torque control. Both devices have low mass ($<$ 0.87 kg), are modular and structurally compliant in selected directions, and are instrumented to measure joint angle and torque. The exoskeletons are actuated by an off-board motor, and torque is controlled using a combination of proportional feedback, damping injection and iterative learning. We tested closed-loop torque control by commanding 50 N·m and 20 N·m linear chirps in desired torque while the exoskeletons were worn by human users, and measured bandwidths greater than 16 Hz and 21 Hz, respectively. During walking trials, we demonstrated 120 N·m peak torque and 2.0 N·m RMS torque tracking error. These performance measures compare favorably with previous devices and with human ankle musculature, and show that these exoskeletons can be used to rapidly explore a wide range of control techniques and robotic assistance paradigms as elements of versatile, high-performance testbeds. Our results also provide insights into desirable properties of lower-limb exoskeleton hardware, which we expect to inform future designs.**

***Index Terms*—Rehabilitation Robotics, Human-Robot Interaction, Ankle Exoskeleton**

I. Introduction

Lower-limb exoskeletons have the potential to aid in rehabilitation [1], assist walking for those with gait impairments [2], reduce the metabolic cost of normal [3] and load-bearing walking [4, 5], improve stability [6] and probe interesting questions about human locomotion [4]. Designing effective lower-limb exoskeletons is a complicated task and may be simplified by assisting a single joint. During normal walking, the ankle produces a larger peak torque and performs more positive work than either the knee or the hip during the stance phase of gait [7]. The ankle joint may therefore prove an effective location for application of assistance.

Many ankle exoskeletons have been designed and built using different approaches to mechanical design, actuation, and control [3–5, 8], but, surprisingly, much still remains unclear about the most effective way to mechanically assist the ankle joint. Much of what has guided design choices for ankle exoskeletons has come from intuition, but some principles of functionality, desirable device properties, and human-robot interactions have emerged. Applying plantarflexor torques about the ankle joint with an external device such that positive work is delivered to the user can reduce metabolic energy cost during normal walking [3] and during walking with heavy loads [9]. Increasing the amount of net work supplied by the device results in a downward trend in metabolic energy cost [10]. Having the ability to apply large torques and net work therefore increases the space of potential assistance techniques. Independent of maximum torque, the responsiveness of the system to changes in desired torques is important. For example, the timing of torque application in the gait cycle strongly affects metabolic energy consumption [11]. The ankle joint also experiences a wide range of velocities during normal walking, with plantarflexion occurring very rapidly. Maximizing the bandwidth of a device, such that it can apply and remove torques quickly, allows it to keep up with the natural movements of the user and enriches the space of potential control strategies.

Although on its own an ankle exoskeleton may have high bandwidth and be capable of withstanding large torques, these features change when a human is added into the loop. One of the main challenges of effective design of ankle exoskeletons is handling this complex human-device interaction. If the goal is to have high torque and high bandwidth then the device must be able to transfer large loads quickly, effectively, comfortably, and safely to the user. Adding series elasticity to the system improves torque control and decouples the human from the inertia of the motor and gearbox [12]. It is worth noting that the optimal stiffness may not be known a priori and may vary across subjects and desired applications. Thus, experiments should be done to help determine the appropriate spring stiffness. Shear forces are not well-supported by the body and often cause discomfort. Applying forces normal to the human, over large surface areas, may allow for the greatest magnitude of applied force while maintaining comfort. Applying forces far from the ankle joint, i.e. increasing the lever arm, reduces the magnitude of applied force necessary for a desired externally-applied ankle torque.

Many ankle exoskeletons are designed with the goal of assisting the human user and reducing overall energy costs. Putting an ankle exoskeleton on the leg, however, automatically incurs a metabolic energy penalty because it adds distal mass [13]. Reducing total device mass helps minimize this incurred penalty. Ankle exoskeletons also interfere with natural movements and, although this problem can partially

This material is based upon work supported by the National Science Foundation under Grant No. IIS-1355716.

[1]Dept. Mechanical Engineering, Carnegie Mellon University, USA.
[2]School of Electric and Electronic Engineering, Nanyang Technological University, Singapore.
[3]Robotics Institute, Carnegie Mellon University, USA.
[*]Corresponding author: S. H. Collins. 5000 Forbes Ave. Pittsburgh, Pennsylvania 15213, USA. Email:stevecollins@cmu.edu

Preprint submitted to 2015 IEEE International Conference on Robotics and Automation. Received October 1, 2014.

be addressed with good control, some interference is unavoidable due to the physical structure of the device. Maintaining compliance in uncontrolled directions allows for less inhibited motion. Reducing the overall envelope of the device, especially the width, lessens penalities incurred from walking with an increased step width [14]. Wearers of the device may vary greatly in anthropometry, such as body mass and leg length. Rather than designing a new device for each user [4], which is time-consuming and expensive, incorporating adjustability or modularity can allow a single exoskeleton to be used on many different subjects.

Human locomotion is a versatile and complex behavior that is still poorly understood, and designing devices to interact usefully with humans during walking is a difficult task. Building adjustable devices with the ability to supply wide ranges of assistive torques using numerous different control schemes provides the freedom to rapidly and inexpensively measure the human response to different assistance strategies. Results from human experiments can provide insights into useful device capabilities and help inform future designs. Our goal was to develop an ankle exoskeleton system, including two custom-designed wearable end-effectors, that demonstrated an effective solution to the problems and challenges inherent in the design of lower-limb exoskeletons.

II. Methods

We designed, built and tested two ankle-foot exoskeleton end-effectors for use with a tethered emulator system. The prototypes, Alpha and Beta, demonstrate two approaches to the challenges in exoskeleton design, including fabrication of strong lightweight components, implementation of series elasticity for improved torque control, and comfortable, adjustable human interfacing. Both devices were designed to reduce interference with natural movements. The Alpha exoskeleton was designed to provide compliance in selected directions, while the Beta exoskeleton was designed to reduce the overall envelope. Bandwidth tests were performed to quantify system-wide closed-loop torque bandwidth, and walking trials were performed to quantify torque tracking error and verify that large torques could be comfortably applied to a human user.

A. Mechanical Design

The ankle exoskeleton end-effectors were actuated by a powerful off-board motor and real-time controller, with mechanical power transmitted through a flexible Bowden cable tether. The motor, controller and tether elements of this system are described in detail in [15].

Both ankle exoskeletons interface with the foot under the heel, the shin just below the knee, and the ground beneath the toe. The exoskeleton frames include rotational joints on either side of the ankle, with axes of rotation approximately collinear with that of the human joint (Fig. 1A). Each frame can be separated into a foot section and shank section (Fig. 1B&C). The foot section has a lever arm that protudes posterior to the ankle joint and wraps around the heel. The Bowden cable pulls upward on this lever while the Bowden cable conduit

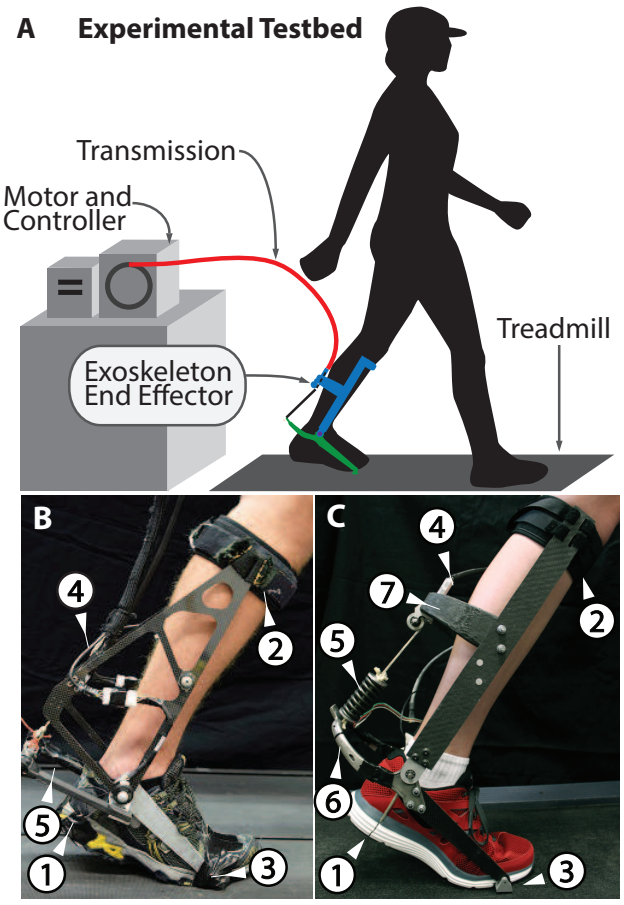

Fig. 1: Emulator system and exoskeleton prototypes. **A** The testbed comprised a powerful off-board motor and controller, a flexible transmission, and an ankle exoskeleton end-effector worn on the person's leg. **B** The Alpha design. Each exoskeleton contacted (1) the heel using a string, (2) the shin using a strap, and (3) the ground using a hinged plate embedded in the shoe. The Bowden cable conduit attached to (4) the shank frame, while the Bowden cable rope terminated at (5) the series spring. **C** The Beta design. In addition to components (1)-(5), this prototype has (6) a titanium ankle lever wrapping behind the heel and (7) a hollow carbon fiber Bowden cable support.

presses downward on the shank section of the frame. This results in an upward force beneath the user's heel, a normal force on the top of the shin, and a downward force on the ground, generating a plantarflexion torque (Fig. 2). The toe and shin attachment points are located far from the ankle joint, maximizing their leverage about the ankle and minimizing the forces applied to the user for a given plantarflexion torque. Forces are comfortably transmitted to the user's shin via a padded strap, which is situated above the calf muscle to prevent the device from slipping down the leg. Forces are transmitted to the user's heel via a lightweight synthetic rope placed in a groove in the sole of a running shoe.

The exoskeletons were designed to provide greater peak torque, peak velocity and range of motion than observed at the ankle during fast walking. The Alpha and Beta devices were designed to withstand peak plantarflexion torques of 120 N·m. The expected peak ankle plantarflexion velocities, which are limited by motor speed, of the Alpha and Beta devices are 300 and 303 deg·s^{-1}, respectively. Both devices have a range of motion of 30° plantarflexion to 20° dorsiflexion, with 0°

Preprint submitted to 2015 IEEE International Conference on Robotics and Automation. Received October 1, 2014.

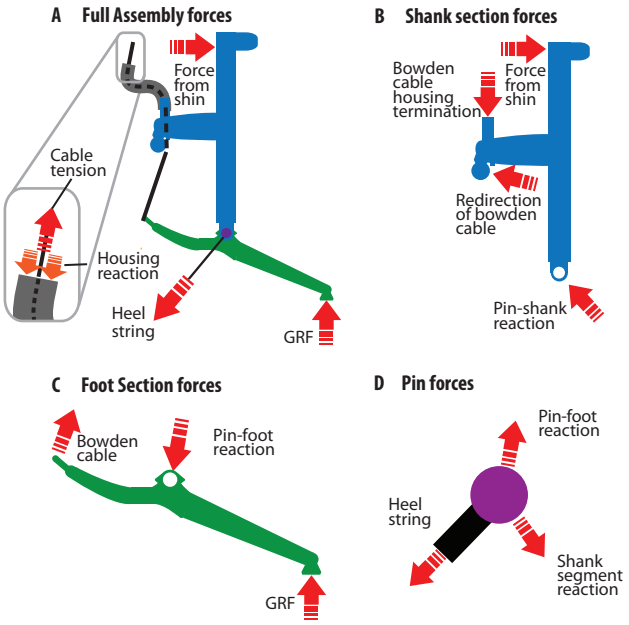

Fig. 2: Free body diagrams of the exoskeleton structure. **A** The complete exoskeleton experiences external loads at the three attachment points, which together create an ankle plantarflexion torque. Forces in the Bowden cable conduit and inner rope (inset) are equal and opposite, producing no net external load on the leg. Free body diagrams depicting loading of **B** the shank segment, **C** the foot segment, and **D** the shaft and heel rope.

corresponding to a natural standing posture.

Both exoskeletons have a modular construction to accommodate a range of subject sizes. Toe struts, calf struts, and heel strings of different lengths can be exchanged to fit different foot and shank sizes. Current hardware fits users with shank lengths ranging from 0.42 to 0.50 m and shoe sizes ranging from a women's size 7 to a men's size 12 (US). Slots in the calf struts allow an additional 0.04 m of continuous adjustability in shank length.

Series elasticity was provided by a pair of leaf springs in the Alpha design and a single coil spring in the Beta design. The leaf springs were custom-designed and made out of fiberglass (GC-67-UB, Gordon Composites, Montrose, CO, USA), which has a mass per unit strain-energy storage, $\rho E \sigma_y^{-2}$, one eighth that of spring steel [15]. A commercially-available coil spring (DWC-225M-13, Diamond Wire Spring Co., Pittsburgh, PA, USA) was used in the Beta design. The leaf springs also made up part of the ankle lever arm in the Alpha exoskeleton, thereby reducing the number of components and saving approximately 0.025 kg compared to the Beta design. This comparison is confounded by factors such as different maximum expected loads and spring stiffnesses.

The choice of spring type had a strong effect on the overall envelopes of the exoskeletons. The structure of the Alpha device extends substantially into the spaces medial and posterior to the ankle joint. This large envelope increased user step width [10], potentially increasing metabolic energy cost during walking [16], and caused occasional collisions with the contralateral limb. The average maximal ankle external rotation during walking for healthy subjects is approximately 18° [17], and the average step width is only 0.1 m [18]. For

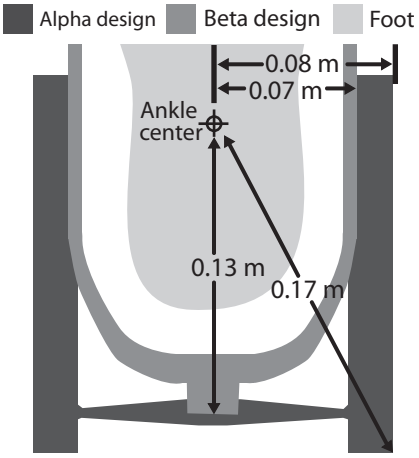

Fig. 3: Comparison of envelopes of the two devices, depicted from above. The Beta device was slimmer in terms of medial-lateral protrusion and maximum protrusion from the joint center.

this reason, the Beta exoskeleton was designed to minimize medial and lateral protrusions to prevent collisions or excessive widening of step width during bilateral use. The maximum protrusion length measured from the center of the human ankle joint is 24% smaller than that of the alpha design (Fig. 3).

The plate-like components of the Alpha design were easily fabricated using machining, while more complex Beta components were better suited to additive manufacturing and lost-wax carbon fiber molding. The ankle lever of the Beta exoskeleton wraps from the medial to the lateral aspects of the user's ankle, with the transmission attached at the rear (Fig. 1). This configuration results in large bending and torsion loads, well-addressed by I-beam and tubular structures, respectively. The Beta ankle lever also required small, precise features for connection to the ankle shaft and toe hardware. Additive manufacturing using electron beam melting of titanium particles allowed these disparate design requirements to be addressed by a single component. The titanium component weighed 0.098 kg less than an equivalent structure from an earlier prototype composed of a carbon fiber ankle lever, two aluminum joint components, and connective hardware. The Bowden cable termination support in the Beta design is subjected to similar loading as the ankle lever, but has less complex connection geometry at the shank struts, making a hollow carbon fiber structure appropriate. This part was manufactured using a variation of the lost wax molding method. A wax form with a threaded aluminum insert was cast using a two-piece fused deposition modeling (FDM) plastic shell-mold. A composite layup was performed on this mold using braided carbon fiber sleeves. The wax was then melted out by submerging the component in warm water. In an earlier prototype, we performed the carbon fiber layup on a hollow plastic mold, reinforced to withstand the vacuum bagging process. This permanent plastic insert added approximately 0.048 kg to the component.

Both exoskeleton designs provide some structural compliance to allow users to invert-evert and internally-externally

Preprint submitted to 2015 IEEE International Conference on Robotics and Automation. Received October 1, 2014.

rotate their ankle joint. Thin plate-like shank struts act as flexures, allowing the calf strap to fit snugly around a wide range of calf sizes and move medially and laterally. This flexural compliance, in concert with sliding of the calf strap on the struts, sliding of the rope beneath the heel, and compliance in the shoe, allows ankle rotation in both roll and yaw during walking. The Bowden cable support connecting the medial and lateral shank struts is located low on the leg in the Alpha design, allowing more deflection at the top of the struts. The Bowden cable support is located higher up in the Beta design to allow space for the in-line coil spring, thereby reducing compliance.

B. Sensing and Control

Both devices sense ankle angle with optical encoders (E4P and E5, respectively, US Digital Corp., Vancouver, WA, USA) and foot contact with switches (7692K3, McMaster-Carr, Cleveland, Ohio, USA) in the heel of the shoe. The Alpha exoskeleton uses a load cell (LC201, Omega Engineering Inc., Stamford, CT, USA) to measure Bowden cable tension. The Beta exoskeleton uses four strain gauges (MMF003129, Micro Measurements, Wendell, NC, USA) in a Wheatstone-bridge on the ankle lever to measure torque directly, presenting a lighter and less expensive solution to accurate force measurement. Bridge voltage was sampled at 5000 Hz and low-pass filtered at 200 Hz to reduce the effects of electromagnetic interference.

Torque was controlled using a combination of classical feedback control and iterative learning. Proportional control with damping injection was used in closed-loop bandwidth tests. An additional iterative learning term was used during walking trials. This approach is described in detail in [19].

For walking tests, desired torque was computed as a function of ankle angle and phase of the gait cycle. During stance, desired torque roughly matched the average torque-angle relationship of the human ankle during normal walking using a method described in detail in [15]. During swing, a small amount of slack was maintained in the Bowden cable, resulting in zero torque.

C. Experimental Methods

To ensure accurate torque measurements, we calibrated torque sensors using suspended weights. The ankle lever was removed and secured upside down in a jig, and torque was incrementally increased by hanging weights of known mass from the Bowden cable. We computed root mean squared error between applied and measured torque from the calibration set.

We performed closed-loop torque bandwidth tests on the ankle exoskeleton while worn by a user. The user's ankle was restrained by a strap that ran under the toe and over the knee (Fig. 4). This captured the effects of compliance at the human-exoskeleton interface on torque control. Linear chirps in desired torque were applied with a maximum frequency of 30 Hz over a 30 second period, and measured torque was recorded. Bode frequency response plots were generated using the Fourier transform of desired and measured torque signals. Ten tests were performed at amplitudes of 20 and 50 N·m, and results were averaged. Bandwidth was calculated as the lesser of the -3 dB cutoff frequency and the 30° phase margin crossover frequency.

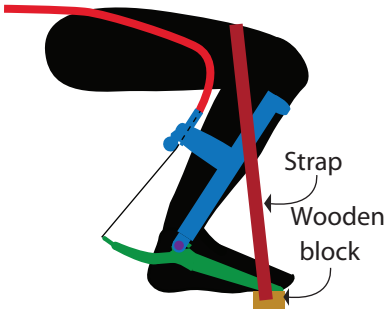

Fig. 4: Bandwidth test setup. The exoskeleton was worn by a human subject, whose leg was restrained using a strap that wrapped over the thigh and attached to a block beneath the toe segment.

Torque tracking performance was evaluated during walking trials with a single healthy subject (1.85 m, 77 Kg, 35 yrs, male). Data was collected over 100 steady-state steps while walking on a treadmill at 1.25 $m \cdot s^{-1}$. Root mean squared error was calculated over the entire trial and for an average step.

III. Results

The total mass of the Alpha and Beta exoskeletons were 0.84 and 0.87 kg, respectively. Torque measurement accuracy tests showed a root mean squared (RMS) error of 0.004 N·m for device Alpha and 0.032 N·m for device Beta (Fig. 5A).

The gain-limited closed-loop torque bandwidths of the Alpha device with 20 N·m and 50 N·m peak torques were 21.1 Hz and 16.7 Hz, respectively (Fig. 5B). The phase-limited bandwidths [20] for the Beta device, at a 30° phase margin, with 20 N·m and 50 N·m peak torques were 24.2 Hz and 17.7 Hz, respectively (Fig. 5B).

In walking trials with device Alpha, the peak of the average measured torque was 80 N·m. The maximum observed torque during pilot tests was 119 N·m. The RMS error for the entire trial was 1.7 ± 0.6 N·m, or 2.1% of peak torque, and the RMS error of the average stride was 0.2 N·m, or 0.3% of peak torque (Fig. 5C). For the Beta device, the peak of the average measured torque was 87 N·m. The maximum observed torque during pilot tests was 121 N·m. The RMS error for the entire trial was 2.0 ± 0.5 N·m, or 2.4% of peak torque, and the RMS error of the average stride was 0.3 N·m, or 0.4% of peak torque (Fig. 5C).

IV. Discussion

Our aim was to design comfortable, modular exoskeletons capable of providing high torque at high bandwidth with accurate torque tracking. Benchmarking experiments demonstrated that the Alpha and Beta exoskeletons compared favorably to similar devices. Weighing less than 0.87 kg, both devices are lighter than powered ankle exoskeletons used for probing the biomechanics of human locomotion [8] or providing assistance during load carriage [9]. The Alpha and Beta devices demonstrated a six-fold increase in bandwith over a pneumatically actuated device that recently reduced metabolic cost below

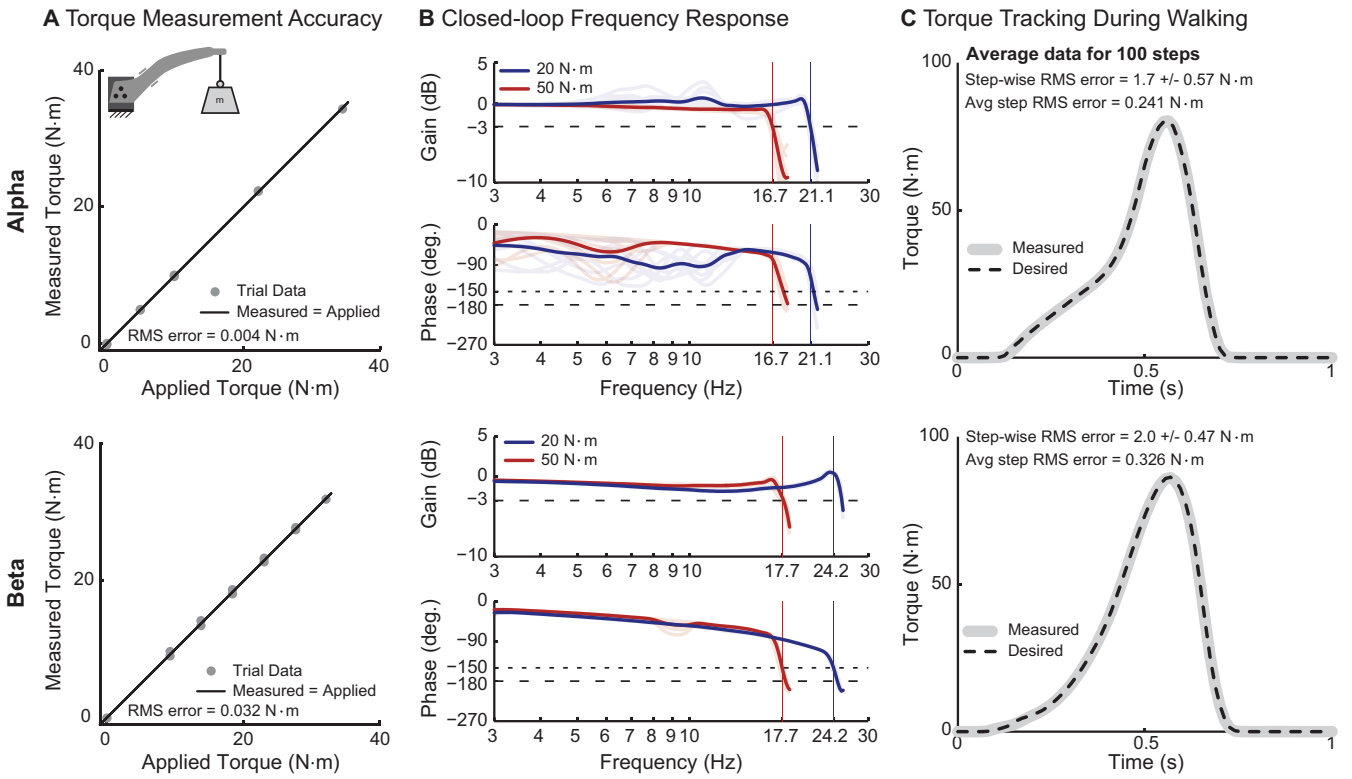

Fig. 5: Experimental results from tests of the Alpha (top) and Beta (bottom) prototypes. **A** Torque measurement calibration results. **B** Bode plots depicting frequency response of the system with peak desired torques of 20 N·m (blue) and 50 N·m (red). Bandwidth was gain-limited for the Alpha device and phase-limited with the Beta device. **C** Average desired and measured torque from 100 steady-state walking steps.

that of normal walking [3]. Comparisons with other platforms are limited due to a lack of reported bandwidth values. In walking tests with users having a large range of shank lengths we observed peak torques of about 120 N·m, comparable to values for similar devices [3, 4, 8]. These results demonstrate robust, accurate torque tracking and the ability to withstand and transfer large, dynamic loads comfortably to a wide variety of human users.

The three-point contact with the user's leg implemented in both exoskeletons provided an effective solution to comfortable, robust interfacing. The locations of the attachment points minimized the magnitude of forces applied to the body, while compliance in selected directions reduced interference with natural motions. Although subtle differences in design choices led to more rigid struts in the Beta exoskeleton than the Alpha exoskeleton, the compliance in the shoe and heel string was sufficient to enable comfortable walking.

Exoskeleton structures with large envelopes may require users to increase step width, resulting in higher metabolic energy consumption [16], and may increase the likelihood of collisions. We found that the envelope of a modular exoskeleton can be reduced by fabricating components with more organic shapes using additive manufacturing and lost-wax carbon fiber layups.

The explicit joints used in the Alpha and Beta designs made measurement of ankle angle simple and accurate. Double shear connections at medial and lateral joints in the Beta design resulted in consistent shaft and encoder alignment. Co-axial single shear joints used in the Alpha design were less robust to loading out of the sagittal plane. Removing the explicit joint from an exoskeleton can reduce overall device weight and envelope while not compromising structural strength [9]. This approach complicates measurement of the ankle angle, however, limiting the number of potential control strategies that can be implemented.

While these exoskeletons are excellent research tools, they cannot be used autonomously. The high torque and bandwidth of these devices are primarily enabled by large off-board motors and controllers. On the other hand, decoupling actuation from end-effector design has allowed rapid design iteration.

The modular nature of these devices allows for accurate alignment of the mechanical joint with the human joint for a wide range of human users. Making components in a variety of sizes and exchanging these components, however, is expensive and time consuming. An adjustable design can reduce these costs, but often adds mass, which increases the effort required to walk with the device [13]. Some designs require orthotists to fabricate custom interfaces for each user [21], which can result in improved fit, but adds to the overhead of subject recruitment.

While leaf springs are theoretically much lighter than coil springs for a given stiffness, in this case they only resulted in a mass-savings of 20% when modified for robustness. The entire ankle lever assembly of the Alpha design, including the two

Preprint submitted to 2015 IEEE International Conference
on Robotics and Automation. Received October 1, 2014.

leaf springs, the aluminum cross-bar, and required connective hardware, actually proved to be 0.048 kg heavier than the titanium ankle lever and coil spring used in the Beta design. This comparison is confounded by the fact that the leaf spring and coil spring have slightly different stiffnesses and that the two exoskeletons were designed for different maximum loads. The Beta exoskeleton originally used a fiberglass leaf spring in place of the coil spring, which made the whole assembly 0.040 kg lighter and lengthened the ankle lever arm, thereby reducing torques at the motor. This leaf spring proved unreliable, however, even after changes were made to the attachment configuration. The coil spring that replaced the leaf spring, though heavier, increased robustness and made interchanging springs of different stiffnesses easier.

Oscillations were present in the bode plot phase diagram for device Alpha at lower frequencies. These may be a result of un-modeled dynamics, particularly those of the tether and the human. Inspection of the time-series torque trajectory showed ripples at lower frequencies that may have been caused by changes on the human-side of the system or oscillations in the Bowden cable transmission. Bandwidth tests could be improved by including more data in the lower frequency range. This could be achieved by commanding an exponential, rather than linear, chirp in desired torque for a longer duration.

Series elasticity plays a large role in torque tracking performance, but optimal spring stiffness may be a function of individual morphology, peak applied torques, and control strategies and might be difficult to predict. In pilot tests with the Beta device, we found that very stiff or very compliant elastic elements worsened torque tracking errors. This was not the case for a prosthetic device we recently developed [22], in which the Bowden cable itself seemed to provide sufficient series compliance. This may be because the prosthesis is in series with the limb, and therefore receives more predictable loading from the user. We plan to perform experiments to characterize these relationships.

V. Conclusion

We designed, manufactured, and tested two ankle-foot exoskeletons which proved to have high peak torque and bandwidth and exceptional torque tracking. These capable devices allow accurate realization of a wide range of complex torque profiles, which will enable exploration of novel assistance strategies. Series elasticity, selective compliance, three-point attachment, form-fitting components, double-shear joints, and powerful off-board motors facilitate effective interactions between the exoskeleton and the user. The same approaches demonstrated here may be implemented in knee and hip exoskeletons, allowing researchers to explore biomechanical interactions across joints during locomotion as well as to analyze the effect of assistance strategies applied to the entire lower limb.

VI. Acknowledgements

The authors thank Jessica Lee, Jan Warnaars, Kristen Hauser and Justin Barsano for their help with design and fabrication of the devices and Padraig Taggart for help editing.

References

[1] S. Jezernik, G. Colombo, T. Keller, H. Frueh, and M. Morari, "Robotic orthosis Lokomat: a rehabilitation and research tool," *Neuromod.*, vol. 6, no. 2, pp. 108–115, 2003.

[2] E. Guizzo and T. Deyle, "Robotics trends for 2012," *Rob. Autom. Mag.*, pp. 119–123, 2012.

[3] P. Malcolm, W. Derave, S. Galle, and D. De Clercq, "A simple exoskeleton that assists plantarflexion can reduce the metabolic cost of human walking," *PLoS: ONE*, vol. 8, no. 2, p. e56137, 2013.

[4] D. P. Ferris, K. E. Gordon, and G. S. Sawicki, "An improved powered ankle-foot orthosis using proportional myoelectric control," *Gait Post.*, vol. 23, pp. 425–428, 2006.

[5] S. Au, M. Berniker, and H. Herr, "Powered ankle-foot prosthesis to assist level-ground and stair-descent gaits," *Neur. Net.*, vol. 21, pp. 654–666, 2008.

[6] M. Kim and S. H. Collins, "Once-per-step control of ankle-foot prosthesis push-off work reduces effort associated with balance during walking," *J. Roy. Soc. Int.*, vol. submitted, 2014.

[7] D. A. Winter, *The Biomechanics and Motor Control of Human Gait: Normal, Elderly and Pathological*. Waterloo, Canada: Waterloo Biomechanics, 1991.

[8] G. S. Sawicki and D. P. Ferris, "Powered ankle exoskeletons reveal the metabolic cost of plantar flexor mechanical work during walking with longer steps at constant step frequency," *The Journal of Experimental Biology*, vol. 212, pp. 21–31, Jan. 2009.

[9] L. M. Mooney, E. J. Rouse, and H. M. Herr, "Autonomous exoskeleton reduces metabolic cost of human walking during load carriage," *J. Neuroeng. Rehabil.*, vol. 11, p. 80, 2014.

[10] R. W. Jackson and S. H. Collins, "The relative benefits of work assistance and otrque assitance in ankle exoskeletons," Boston, USA, 2014.

[11] P. Malcolm, R. E. Quesada, J. M. Caputo, and S. H. Collins, "The influence of push-off timing in a robotic ankle-foot prosthesis on the energetics and mechanics of walking."

[12] G. Pratt and M. Williamson, "Series elastic actuators," in *Proc. Int. Conf. Intel. Rob. Sys.*, 1995.

[13] R. C. Browning, J. R. Modica, R. Kram, and A. Goswami, "The effects of adding mass to the legs on the energetics and biomechanics of walking," *Med. Sci. Sports Exer.*, vol. 39, no. 3, pp. 515–525, 2007.

[14] J. M. Donelan, Q. Li, V. Naing, J. A. Hoffer, D. J. Weber, and A. D. Kuo, "Biomechanical energy harvesting: Generating electricity during walking with minimal user effort," *Science*, vol. 319, no. 5864, pp. 807–810, 2008.

[15] J. M. Caputo and S. H. Collins, "A universal ankle-foot prosthesis emulator for experiments during human locomotion," *J. Biomech. Eng.*, vol. 136, p. 035002, 2014.

[16] J. M. Donelan, R. Kram, and A. D. Kuo, "Mechanical and metabolic determinants of the preferred step width in human walking." *Proc. Roy. Soc. Lon. B*, vol. 268, pp. 1985–1992, 2001.

[17] M. P. Kadaba, H. K. Ramakrishnan, and M. E. Wootten, "Measurement of lower extremity kinematics during level walking," *Journal of Orthopaedic Research*, vol. 8, pp. 383–392, 1990.

[18] T. M. Owings and M. D. Grabiner, "Variability of step kinematics in young and older adults," pp. 24–29, 2004.

[19] J. Zhang, C. C. Cheah, and S. H. Collins, "A systematic comparison of nine prominent torque control methods in a tethered ankle exoskeleton with series elastic actuation during human walking," *Int. J. Rob. Res.*, vol. submitted, 2014.

[20] "Telecommunications: Glossary of telecommunication terms," *Federal Standard 1037C*, Aug. 1996.

[21] K. E. Gordon, D. P. Ferris, and A. D. Kuo, "Metabolic and mechanical energy costs of reducing vertical center of mass movement during gait," *Arch. Phys. Med. Rehab.*, vol. 90, pp. 136–144, 2009.

[22] J. M. Caputo and S. H. Collins, "An experimental robotic testbed for accelerated development of ankle prostheses," in *Proc. Int. Conf. Rob. Autom.*, 2013, pp. 2630–2635.